Fiber-Crawling Microrobots

S. Challa, M. S. Islam, and C.K. Harnett

Abstract—**Microrobots that crawl along fibers can work as linear actuators and as active components in assembling 3D structures from microscale parts. They are also a potential topic for microrobotics demonstrations and competitions, analogous to contests in the macroscale rope-climbing robot domain. In this work, we briefly review cable-traveling robots, then demonstrate a magnetically driven wire crawler where the wire provides the driving power, causing the robot to vibrate. Stick-and-slip friction creates motion along the wire. We discuss scaling down both the magnetic actuator and the flexible contacts that produce stick-and-slip motion. Two types of compliant frictional contacts are demonstrated: a thin plastic film, and at a smaller scale, anisotropic microbristles made from natural materials. Lastly, we discuss a path to further miniaturization.**

I. Introduction

In nature, the challenges of one-dimensional (1-D) locomotion on fiber structures are tackled by spiders on webs and parasites on hair and plant stems. 1-D locomotion inside hollow structures is the specialty of cancer cells in capillaries and other lumens during metastasis. At an even smaller scale, muscles contract and microtubules control cell shape thanks to specialized molecules that crawl on fibers.

In the engineering world, a fiber provides a solution to powering and locating a micro robot (at least in one dimension), and getting signals to and from it. Fibers working as conductive wires or performing other functions can also be part of a finished object, with microcomponents positioned along a wire in a composite structure. Fine (20-50 micron diameter) wire-bonding wires used in IC packaging could potentially support and power electronic components while giving 360 degree access to cooling airflows.

Flipping the concept of fiber-crawling microrobots upside down, stationary microrobots that can manipulate fibers are needed to handle delicate vessels in microsurgery and biological research [1], to perform mechanical testing and analysis on fibers in the paper and textile industry [2], and to assemble electronic devices from nanotubes and nanowires. Most often, fiber manipulation is done by opening and closing grippers. Methods that replace these sequential operations with vibration, or another continuous driving method, could lead to parallelization and scale-up. Combining these ideas, a robot crawling on a fiber and manipulating a second fiber could form the basis for a microtubule-like system that builds reconfigurable 3-D microstructures.

At a larger scale, fiber- and cable-traversing systems are an established category in robotics, and climbing robots are a staple of robotics competitions. Applications cover signal cable and structural cable inspection [3], and construction, for example using an existing line to guide the installation of new line in parallel. Pipe crawlers, for residential plumbing and oil pipeline inspection cover a similar 1-D domain and use some of the same locomotion methods. Locomotion methods for rope and cable climbers often use driven pulleys or wheels. A common method that is more suitable for miniaturization is sequential clamping combined with extension.

At the centimeter and larger scale, cable clamping has been driven by pistons [4] and gears [5]. However, rotating and sliding parts do not scale down well for microrobots. Below ~1 cm, compliant mechanisms are more compatible with friction and adhesion forces. The equivalent of sequential clamping at the microscale is stick-and-slip motion, usually transmitted from the robot to the surface by bristles or microsprings. Actuators for driving microrobots include electrostatic [6,7], magnetic [8,9], piezoelectric, and phase-changing materials [10].

Vibration from such local actuators [11], from externally applied magnetic fields [12,13] and from laser heating [14] has been used to generate linear [15] and multi-axis [16,17] motion in microrobots.

While actuators driven from on-board power sources, local energy extracted from the chemical environment [18], or externally applied fields could supply power and control a small wire crawler, we chose to use the wire to generate magnetic fields for vibrating a small permanent magnet on a crawler designed for stick-slip motion. Not only was the crawler guaranteed to be near its wire, eliminating the problem of focusing the driving signal, but magnetic fields also offered bidirectional control with a single conductor by changing the direction of the current. In this work, we investigated the system's velocity as a function of driving frequency and contact materials.

II. Magnetic Forces Near Current-Carrying Wires

A. Analysis of force exerted on a permanent magnet by a current-carrying wire

A wire carrying a current generates a circulating magnetic field that will create vibration by pushing and

* This research effort was supported by U.S. National Science Foundation Award 1828355, "Development of a Multiscale Additive Manufacturing Instrument with Integrated 3D Printing and Robotic Assembly," and performed in part at the Micro/Nano Technology Center (MNTC). The MNTC is a member of the National Science Foundation Manufacturing and Nano Integration Node, supported by ECCS-1542174.

All authors are with the Department of Electrical and Computer Engineering, University of Louisville, Louisville, KY 40292 USA (Corresponding author C. K. Harnett e-mail: c0harn01@louisville.edu).

978-1-7281-0948-0/19/$31.00 ©2019 IEEE

pulling a small permanent magnet away from or toward the wire axis. The magnetic field $\boldsymbol{H}$ from a wire carrying a current I is

$$\boldsymbol{H} = \frac{I}{2\pi\rho}\,\hat{\boldsymbol{\varphi}} \qquad (1)$$

where ρ is the perpendicular distance from the wire, and $\hat{\boldsymbol{\varphi}}$ is the azimuthal direction given by the right-hand rule. A permanent magnet with magnetic moment $\boldsymbol{m}$ has a potential energy

$$U = \boldsymbol{m} \cdot \mu\boldsymbol{H} \qquad (2)$$

where $\boldsymbol{m}$ is the magnet volume v times the remanent magnetic field B_r of the material, divided by its magnetic permeability μ. (For a NdFeB magnet, the magnetic permeability is fairly close to the permeability of free space, 1.05 μ_0 .) In our design, the magnet always has its dipole moment aligned along positive or negative $\hat{\boldsymbol{\varphi}}$. Treating the magnet as a point dipole at a distance ρ from the wire axis, the dot product is approximately

$$U = \pm\frac{vB_rI}{2\pi\rho}, \qquad (3)$$

depending on whether the magnet is parallel (-) to the magnetic field from the wire, or antiparallel (+). The force on the magnet is the negative gradient of the potential energy:

$$\boldsymbol{F} = \pm\frac{vB_rI}{2\pi\rho^2}\hat{\boldsymbol{\rho}} \qquad (4)$$

where a parallel magnet (-) is pulled toward smaller values of ρ at the wire axis, and an antiparallel magnet is repelled from the wire. The force is strongest at the wire surface (ρ= 80 microns for the 34-gauge wire used in the following experiments).

B. Driving circuit

Figure 1 shows the method for driving periodic electric currents that generate magnetic fields around the wire supporting the crawler.

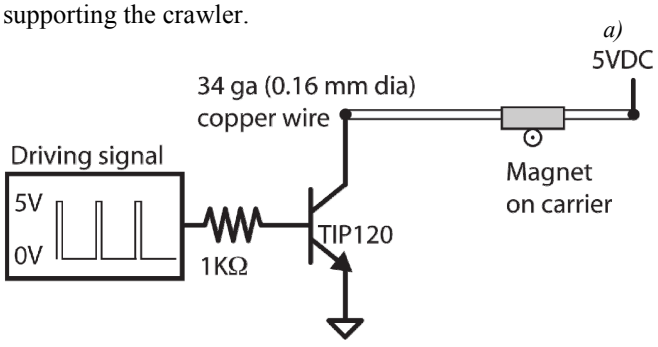

Figure 1: Schematic of magnetic crawler driving circuit.

To drive current through the wire and create an azimuthal magnetic field, a 5V, 24W power supply (Kaga Electronics KTPS24-05040WA-VI-P1, USA) was grounded momentarily using a power transistor (TIP120) driven by a 5V signal from a computer. After the magnetic crawlers were threaded onto the wire, the ends of the wire were soldered to header pins. The wires were tightened to form horizontal tracks by plugging the header pins into a solderless breadboard. While the driving signal was 5V, currents of 2A were drawn through 20 cm of the 34-gauge magnet wire, attracting the magnet toward the wire. With the driving signal off, the magnet fell away from the wire due to gravity.

III. Magnetically Driven Crawler Designs

A. Centimeter-scale crawler

Figure 2 shows a centimeter-scale asymmetric magnetic crawler. A NdFeB magnet made from two stacked discs (1.58 mm diameter, 0.79 mm thick, K & J Magnetics, Inc.) was attached to a 0.005" thick, asymmetric V-shaped polyester carrier with overall length of ~1 cm. The carrier was threaded onto the wire. Stick-slip motion occurred as the magnet moved toward the wire because of the magnetic field, and away from the wire because of gravity. The flexibility of the thin polyester, illustrated schematically in Figure 2, likely contributed to stick-slip motion by allowing the two ends of the crawler to change their separation during a cycle. Pivoting at the far end from the magnet (right side), followed by slipping because of its smaller normal force compared to the left side of the crawler, would produce the observed leftward motion.

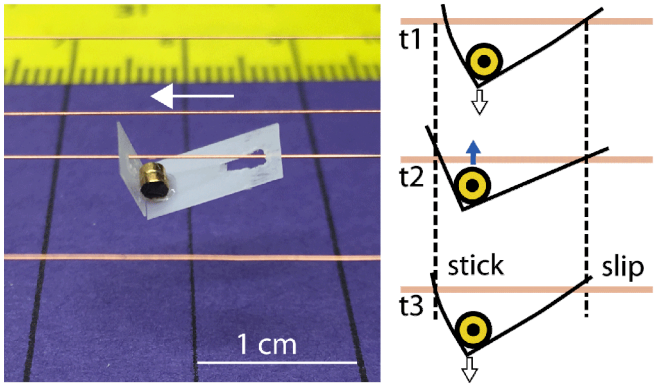

Figure 2: Left: Centimeter-scale wire crawler with arrow showing direction of current and motion; Right: stick-slip sequence; magnetic moment is pointing out of the page.

This device moved in the direction shown in Figure 2 (left) with a top speed of 1.4 mm/second at a driving frequency of 100 Hz with a 10% duty cycle. Measurements were taken with a horizontal wire as measured by a bubble level. From 10 to 120 Hz, velocities were in the 1 mm/s range; at 100 Hz each step of the cycle illustrated in Figure 2 corresponded to approximately 14 microns. At higher frequencies than 120 Hz, it oscillated slowly and showed little net motion. Changing the direction of the current to repel instead of attract the magnet did not produce any motion.

B. Millimeter-scale crawler

To scale down the stick-and-slip motion using smaller compliant features, we surveyed plant and insect parts, mammalian hairs, and bird feathers as prototyping materials.

Bird feathers are examples of soft, anisotropic materials that have aligned and regular bristles at a microscopic size scale. To construct a crawler lined with feather "bristles," a magnet was glued on a 1 mm diameter wire coil filled with goose down filaments. The small gaps in the wire coil (80-100 microns) allowed glue to adhere the feathers from the outside without filling the tube. Feathers are constructed from keratin, which has a lower modulus (2.5 GPa) than the Mylar polyester sheet used in the centimeter-scale crawler (4-5 GPa). However, the structure of feathers is more important than the bulk material properties in determining their mechanical behavior [19]. Goose down is made from fibers having anisotropic barbs [20]. These secondary and tertiary structures (Figure 3) are aligned in a direction that we observed to produce motion toward the quill end of the feather.

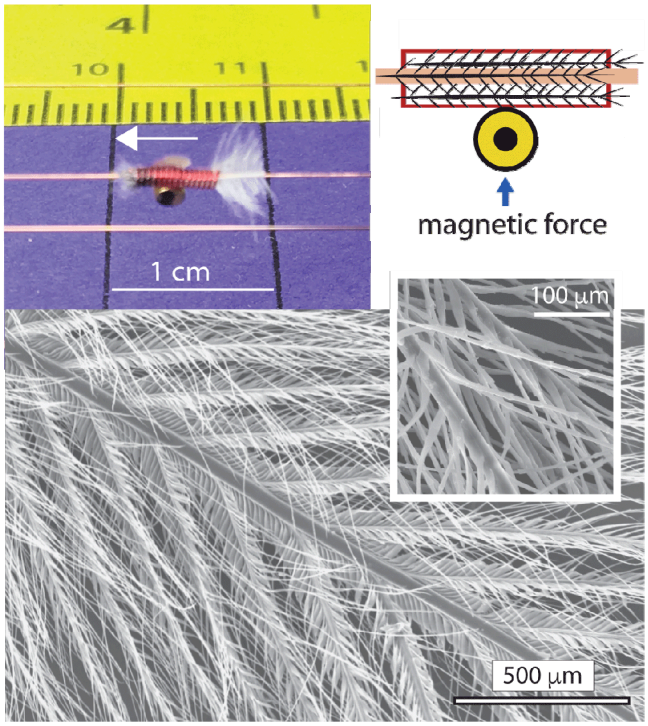

Figure 3: Millimeter-scale crawler (top), lined with goose down filaments. Bottom: scanning electron micrograph of the goose down used in these experiments, showing barbs branching off the main stem and inset showing tertiary nodes on barbules.

Maximum speeds were seen at driving frequencies between 50 and 200 Hz at a 10% duty cycle. Like the centimeter-scale crawler, no net motion was seen when the magnet was repelled from the wire, only when the current was set in the direction that attracted the magnet.

When the current was set to repel the magnet, the stiff metal wire of the tube prevented further vertical motion away from the wire. This observation led us to create pairs of crawlers with oppositely oriented magnets and connect them with thread. By changing the direction of the current, we saw that one of the crawlers could be activated, attracted to the wire and vibrating, while the other crawler was repelled from the wire and stayed "off," moving at a smaller amplitude only because of mechanical coupling to the driven actuator [21,22]. Connecting such a pair of crawlers might offer a way to control the position of a compound micro crawler, moving it to a specific location on a wire by adjusting both the sign and frequency of the driving signal.

Because the lining was a natural material with variations, several feather-lined crawlers were built and tested, as well as a control that had no feathers. Most attained velocities in the 3- to 7- millimeter per second range (Figure 4), except for the feather-free control device, which oscillated but did not experience much net motion.

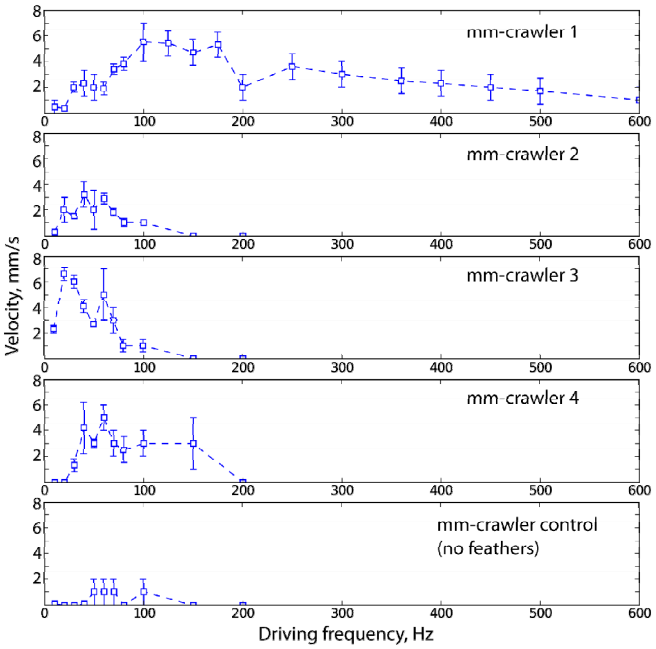

Figure 4: Velocity *vs.* frequency for four similar feather-lined millimeter-scale crawlers, and lastly a control with no feathers

All the crawlers (except the feather-free tube) moved toward the quill end of the feathers, and all moved at least twice as fast as the centimeter-scale crawler.

The main cause of a slow crawler was too much material lining the tube. Removing filaments was observed to suddenly speed up a crawler as long as there was still some inner lining left. Optimal filling or an especially well-aligned barb structure might be the cause of the fast, high frequency crawler in the top plot and pictured in the Figure 3 photo. These prototypes suggest a thin lining of microfabricated, aligned structures resembling the 5-micron diameter barbules of Figure 3 could lead to fast, uniform, small-scale wire crawlers.

IV. Scaling to Smaller Sizes

A. Magnetic Force Scaling

Scaling down the system is only possible if magnetic forces continue to dominate other forces at the microscale.

Magnetic force scales directly with magnet volume (Equation 4). Exerting force on permanent magnets requires the applied magnetic field to have a spatial gradient, while exerting torque does not. For free and untethered robots, driving with torque is preferable to gradient as one scales down [23]. However, that analysis considered open domains where the larger the domain, the more power must be pumped into electromagnets to generate a sufficient spatial gradient over the robot's operating volume. Here we keep the robot confined near the wire surface, where there is a strong gradient, especially for a thin wire.

As magnets scale down in size, there is not enough material to lock in a permanent dipole moment in the face of thermal fluctuations. The smallest permanent magnet reported is 5 nm diameter [24] with similar properties to NdFeB, stable up to ~500 C. However, long before magnet diameters reach the submicron range, adhesion forces begin to dominate. For a NdFeB sphere of radius a, as a gets smaller, at some point the repelling force in Equation 4 will be insufficient to overcome surface adhesion forces. One can improve things by increasing the wire current and therefore the applied magnetic field. As long as the field stays lower than about twice the magnetic material's intrinsic coercivity (H_{ci} = 955 kA/m for NdFeB grade N42) the permanent magnet will not become remagnetized by the applied magnetic field. With the single thin wire in this system, the field does not come close to the remagnetization level because of thermal limitations. The wire's surface temperature must stay well below the Curie temperature of the permanent magnet, which for NdFeB is 310 C, and also below the burn-off temperature of the enamel, around 200 C. For the 34-gauge wire used in the experiments, the DC current must stay less than 2 Amperes to satisfy this condition.

Figure 5 shows that in this case, typical few-micro Newton particle adhesion forces [25] will exceed magnetic forces at magnet diameters of 60 microns and below. Coatings and contact-prevention strategies might allow smaller magnets to be used.

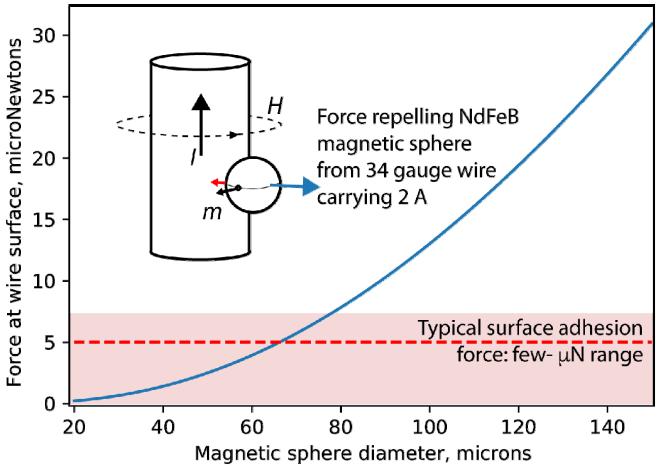

Figure 5: Scaling down magnetic materials leads to small forces (proportional to magnet volume) that must compete with surface adhesion

B. Microscale crawler placement

Below the millimeter scale, automated assembly methods are needed to both build and place crawlers on wires. Other groups have successfully assembled microrobots incorporating small (sub-300 micron side length) rare earth magnets [26, 27]. Here we instead investigated the problem of threading crawler bodies onto fine wires using microfabrication techniques.

Strain-engineered gripper arms pop up from a silicon wafer with a radius of curvature based on the thickness of the thin-film layers, and other material properties [28]. We adjusted them to grasp onto copper magnet wire in Figure 6. A 400 nm thick thermal oxide layer was grown on silicon wafers by wet oxidation in a tube furnace at 1000 C. Then, a 130 nm thick chromium layer was deposited on the oxidized wafer using a sputtering machine (Lesker PVD75) to sputter coat the wafers from a chromium target with 300 W DC power, 5 mTorr argon pressure and 8-10 minutes of deposition time. Cr patterning was done with standard photolithography and etching techniques. Oxide etching was done to pattern the oxide using the Cr layer as a mask; etching was carried out in a March plasma etcher for 10 minutes with 240 mTorr pressure of CF_4:H_2 at a partial pressure ratio of 60:40 and a RF power of 260 W. Strain-mismatched bilayer patterns are thereby created. A copper wire was placed on the surface and aligned with array of gripper structures in a column by sliding a 79 micron diameter 40 AWG insulated Cr wire through 1.2 mm diameter holes etched through deep reactive ion etching in alignment with the gripper features. The structures were released using a XeF_2 etch chamber. (Xactix, Inc.) to undercut them from the silicon wafer. The bilayer curled and grasped onto the copper wire to minimize its stored strain energy. The theoretical radius of curvature of the bilayers is 142 ± 5 microns [29]. For grippers with arm lengths in the range of 200-500 microns, the etch process required 30 or more 30s cycles of exposure to an atmosphere of 3 Torr XeF_2 for complete release from the silicon wafer.

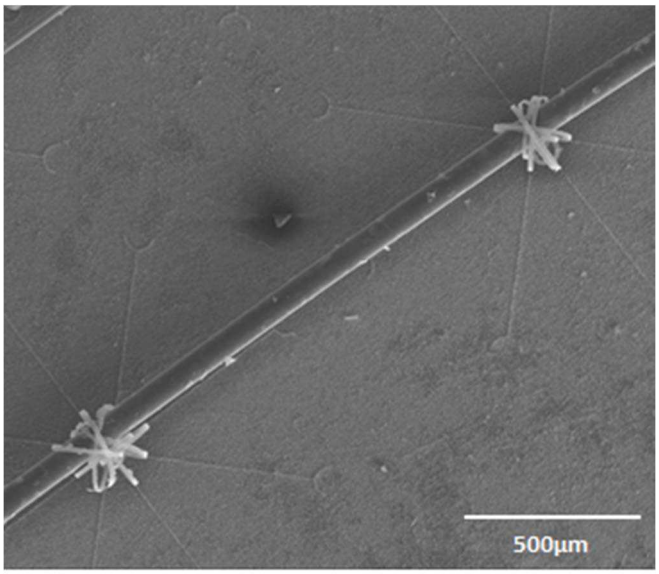

Fig 6: Grippers of diameter 297 ± 20 microns on a 40 AWG copper wire of diameter 79 microns.

Magnets could be added to the process using thin-film or paste-stenciling techniques followed by alignment in magnetic fields. Alternatively, a robotic microassembly system might attach magnets to the gripper structures while they are still planar [30]. The last few steps of the fabrication process do not involve high temperatures or etchants that would damage magnets. It is likely that permanent magnets could be incorporated near the end of this process as they have been in other MEMS processes, making further miniaturization possible.

These thin, compliant structures are also good candidates for engineering stick-slip structures resembling the feathers of Figure 3, with better device-to-device uniformity.

V. Discussion and Conclusions

In this work, we demonstrated a wire crawler powered by a magnetic field from the wire. Interaction between compliant angled structures and the wire surface were responsible for transforming toward-wire magnet motion into translation along the wire. While a bendable polyester sheet exhibited some stick-and-slip motion, faster speeds were obtained with hierarchically structured goose down feathers. Microfabricated structures imitating those shapes are likely to produce more uniform results than what we obtained using natural materials.

Two-direction systems would offer more options for controlling a crawler's location and performing tasks. These goals might be achieved by tethering a pair of opposed crawlers and adjusting the polarity of the current to activate one or the other. Depending on the application, it might also be acceptable to have multiple parallel conductors on a wire, so a crawler could work with voltage differences. However, a single-wire design in this paper makes it simpler to apply microfabrication-based assembly techniques such as strain-engineered fiber grippers.

Returning to a nature-inspired theme, many examples of fibers given in the introduction to this paper have specialized surface features: spikes on plant stems, ridges on animal hairs, and the directional texture on microtubules that motor proteins can detect [31]. Adding such features to a microcrawler-and-fiber system might help researchers develop vibrational actuators that can better navigate biological terrain or manipulate natural microfibers.

References

[1] R. Wierzbicki *et al.*, "Design and fabrication of an electrostatically driven microgripper for blood vessel manipulation," *Microelectron. Eng.*, vol. 83, no. 4, pp. 1651–1654, Apr. 2006.

[2] P. Saketi and P. Kallio, "Microrobotic platform for making, manipulating and breaking individual paper fiber bonds," in *2011 IEEE International Symposium on Assembly and Manufacturing (ISAM)*, 2011, pp. 1–6.

[3] K. H. Cho, Y. H. Jin, H. M. Kim, H. Moon, J. C. Koo, and H. R. Choi, "Caterpillar-based cable climbing robot for inspection of suspension bridge hanger rope," in *2013 IEEE International Conference on Automation Science and Engineering (CASE)*, 2013, pp. 1059–1062.

[4] Y. C. Koo, A. B. Elmi, and W. A. F. Wajdi, "Piston Mechanism Based Rope Climbing Robot," *Procedia Engineering*, vol. 41, pp. 547–553, Jan. 2012.

[5] S. Urankar, P. Jain, A. Singh, A. Saxena, and B. Dasgupta, "Robo-Sloth: A Rope-Climbing Robot," *Department of Mechanical Engineering, Indian Institute of Technology*, pp. 1–10, 2003.

[6] Ethan W. Schaler, Loren Jiang, Caitlyn Lee, Ronald S. Fearing, "Bidirectional, Thin-Film Repulsive-/Attractive-Force Electrostatic Actuators for a Crawling Milli-Robot," in *2018 International Conference on Manipulation, Automation and Robotics at Small Scales (MARSS)*.

[7] Nianfeng Wang, Chaoyu Cui, Bicheng Chen, and Xianmin Zhang, "Design and Analysis of Bistable Dielectric Elastomer Actuator with Buckling Beam," in *2018 International Conference on Manipulation, Automation and Robotics at Small Scales (MARSS)*.

[8] E. Diller and M. Sitti, "Micro-Scale Mobile Robotics," *Foundations and Trends® in Robotics*, vol. 2, no. 3, pp. 143–259, 2013.

[9] A. Hsu, A. Wong-Foy, and R. Pelrine, "Ferrofluid Levitated Micro/Milli-Robots," in *2018 International Conference on Manipulation, Automation and Robotics at Small Scales (MARSS)*, 2018, pp. 1–7.

[10] U. Rembold, S. Fatikow, T. H. Dörsam, and B. Magnussen, "The Use of Actuation Principles for Micro Robots," in *Ultimate Limits of Fabrication and Measurement*, M. E. Welland and J. K. Gimzewski, Eds. Dordrecht: Springer Netherlands, 1995, pp. 33–40.

[11] K.-M. Lee, Y. Kim, J. K. Paik, and B. Shin, "Clawed Miniature Inchworm Robot Driven by Electromagnetic Oscillatory Actuator," *J. Bionic Eng.*, vol. 12, no. 4, pp. 519–526, Dec. 2015.

[12] D. R. Frutiger, K. Vollmers, B. E. Kratochvil, and B. J. Nelson, "Small, Fast, and Under Control: Wireless Resonant Magnetic Micro-agents," *Int. J. Rob. Res.*, vol. 29, no. 5, pp. 613–636, Apr. 2010.

[13] J. Lee, Y. S. Lee, and W. Park, "ViMbot: Design and control of a new magnet robot actuated by an external vibrating magnetic field," in *2015 IEEE International Conference on*

Robotics and Automation (ICRA), 2015, pp. 5358–5363.
[14] M. R. Pac and D. O. Popa, "3-DOF untethered microrobot powered by a single laser beam based on differential thermal dynamics," *IEEE Int. Conf. Robot. Autom.*, 2011.
[15] F. Becker, S. Boerner, V. Lysenko, and I. Zeidis, "On the mechanics of bristle-bots-modeling, simulation and experiments," *ISR/Robotik 2014;*, 2014.
[16] L. Giomi, N. Hawley-Weld, and L. Mahadevan, "Swarming, swirling and stasis in sequestered bristle-bots," *Proceedings of the Royal Society A: Mathematical, Physical and Engineering Sciences*, Mar. 2013.
[17] W. P. Weston-Dawkes, A. C. Ong, M. R. A. Majit, F. Joseph, and M. T. Tolley, "Towards rapid mechanical customization of cm-scale self-folding agents," in *2017 IEEE/RSJ International Conference on Intelligent Robots and Systems (IROS)*, 2017, pp. 4312–4318.
[18] J. L. Moran, "7 - Robotic colloids: Engineered self-propulsion at the microscale (and smaller)," in *Robotic Systems and Autonomous Platforms*, S. M. Walsh and M. S. Strano, Eds. Woodhead Publishing, 2019, pp. 129–177.
[19] R. Bonser and P. Purslow, "The Young's modulus of feather keratin," *J. Exp. Biol.*, vol. 198, no. Pt 4, pp. 1029–1033, 1995.
[20] M. E. Fuller, "The structure and properties of down feathers and their use in the outdoor industry," Ph.D. thesis, University of Leeds, 2015.
[21] URL: "Slow motion magnetic wire crawler – Left Magnet," https://youtu.be/oo4DKKSbW7o Accessed: April 7, 2019
[22] URL: "Slow motion magnetic wire crawler- Right Magnet," https://youtu.be/A8Gc-65BG14 Accessed: April 7, 2019
[23] J. J. Abbott *et al.*, "How Should Microrobots Swim?," *Int. J. Rob. Res.*, vol. 28, no. 11–12, pp. 1434–1447, Nov. 2009.
[24] A. A. El-Gendy, M. Bertino, D. Clifford, M. Qian, S. N. Khanna, and E. E. Carpenter, "Experimental evidence for the formation of CoFe2C phase with colossal magnetocrystalline-anisotropy," *Appl. Phys. Lett.*, vol. 106, no. 21, p. 213109, May 2015.
[25] R. Jones, H. M. Pollock, J. A. S. Cleaver, and C. S. Hodges, "Adhesion Forces between Glass and Silicon Surfaces in Air Studied by AFM: Effects of Relative Humidity, Particle Size, Roughness, and Surface Treatment," *Langmuir*, vol. 18, no. 21, pp. 8045–8055, Oct. 2002.
[26] C. Pawashe, S. Floyd, and M. Sitti, "Multiple magnetic microrobot control using electrostatic anchoring," *Appl. Phys. Lett.*, vol. 94, no. 16, p. 164108, Apr. 2009.
[27] W. Jing, N. Pagano, and D. J. Cappelleri, "A novel micro-scale magnetic tumbling microrobot," *J Micro-Bio Robot*, vol. 8, no. 1, pp. 1–12, Feb. 2013.
[28] E. Moiseeva, Y. M. Senousy, S. McNamara, and C. K. Harnett, "Single-mask microfabrication of three-dimensional objects from strained bimorphs," *J. Micromech. Microeng.*, vol. 17, no. 9, p. N63, Aug. 2007.
[29] S. Challa, C. Ternival, S. Islam, J. Beharic, and C. Harnett, "Transferring Microelectromechanical Devices to Breathable Fabric Carriers with Strain-Engineered Grippers," *MRS Advances*, pp. 1–8.
[30] A. N. Das, P. Zhang, W. H. Lee, D. Popa, and H. Stephanou, "μ3: Multiscale, Deterministic Micro-Nano Assembly System for Construction of On-Wafer Microrobots," in *Proceedings 2007 IEEE International Conference on Robotics and Automation*, 2007, pp. 461–466.
[31] J. Howard and A. A. Hyman, "Preparation of marked microtubules for the assay of the polarity of microtubule-based motors by fluorescence microscopy," *Methods Cell Biol.*, vol. 39, pp. 105–113, 1993.